

Overtone Transition $2\nu_1$ of HCO^+ and HOC^+ : Origin, Radiative Lifetime, Collisional Quenching

Miguel Jiménez-Redondo,^{[a]+} Liliia Uvarova,^{[b]+} Petr Dohnal,^[b] Miroslava Kassayová,^[b] Paola Caselli,^[a] Pavol Jusko^{*[a]}

We present spectra of the first overtone vibration transition of C–H/ O–H stretch ($2\nu_1$) in HCO^+ and HOC^+ , recorded using a laser induced reaction action scheme inside a cryogenic 22 pole radio frequency trap. Band origins have been located at 6078.68411(19) and 6360.17630(26) cm^{-1} , respectively. We introduce a technique based on mass selective ejection from the ion trap for recording background free action spectra. Varying the number density of the neutral action scheme reactant (CO_2 and Ar, respectively) and collisional partner reactant inside the ion trap, permitted us to estimate the radiative lifetime of the state to be 1.53(34) and 1.22(34) ms, respectively, and the collisional quenching rates of $\text{HCO}^+(2\nu_1)$ with He, H_2 , and N_2 .

Introduction

The formyl cation, HCO^+ , is an abundant molecule in the interstellar medium, being first detected already more than 50 years ago, interestingly under the name “X-ogen”,¹ prior to its laboratory identification.² Although the existence of its higher energy isomer isoformyl cation, HOC^+ , was clear, its microwave spectrum was only measured in a dc glow discharge a decade later,³ and its interstellar detection quickly followed. The study by Woods *et al.*⁴ focused on searching for HOC^+ in 14 interstellar sources, successfully detected HOC^+ towards Sgr B2, and was even able to estimate the ratio of $[\text{HCO}^+]/[\text{HOC}^+] \approx 375$. $\text{HCO}^+/\text{HOC}^+$, together with HCN/HNC , are the two most simple linear closed shell isomeric systems, playing a crucial role in astrophysics, as well as in fundamental molecular physics, i.e., properties of molecular ions. Of the two isomers, HCO^+ is energetically more favourable compared to HOC^+ , with the ground states separated by 1.74 eV (from proton affinities on O and C, respectively⁸), and the isomerisation barrier from $\text{HOC}^+ \rightarrow \text{HCO}^+$ is 1.52 eV.⁹ The energy diagram of levels within both isomers can be seen in Fig. 1.

The Woods *et al.*² study was the first to perform ground rotational spectroscopy on HCO^+ in a discharge. IR spec-

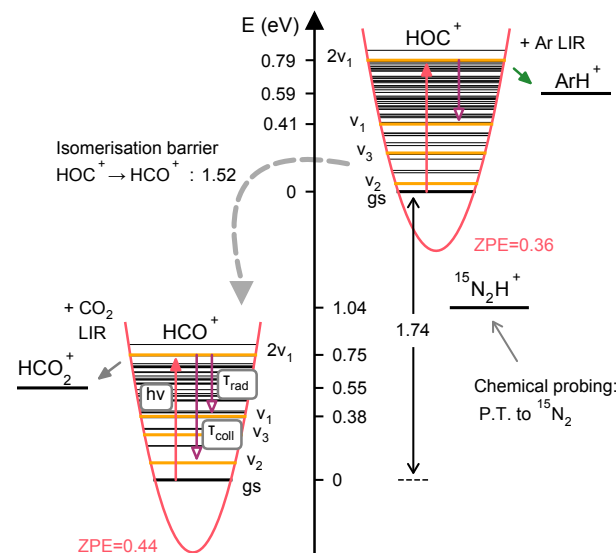


Figure 1. Energy level diagram for HCO^+ and HOC^+ ions. The vibrational energy levels are calculated from HCO^+ ⁵ and HOC^+ ⁶ spectroscopic constants, the zero point energies are taken from ref.⁷ The red arrows represent the induced photon excitation, the magenta arrows radiative and collisional deexcitation. The gray, green arrows represent the LIR reaction pathways to HCO_2^+ and ArH^+ , respectively. The HCO^+ does not proton transfer to $^{15}\text{N}_2$, unless sufficiently excited. See text for details.

troscopy, first determining ν_1 ,¹⁰ then also reporting rotationally resolved P, R branches therein,¹¹ the bending mode ν_2 ^{12,13} and C–O stretch ν_3 ,¹⁴ quickly followed. The radiative lifetime of HCO^+ in the ν_1 state¹⁵ and in the bending mode ν_2 up to 8, has been studied using an ICR trap.¹⁶ Newer experimental studies, after 2000, focused on higher excited vibrational states, e.g., the determination of ν_2 , x_{22} , g_{22} , and $B(030)$,¹⁷ and the acquisition of the pure rotational spectrum of HCO^+ up to 1.2 THz.¹⁸ More recently, the ν_1 band has been re-inspected in high resolution with the help of a frequency comb,¹⁹ and finally, Neese *et al.*⁵ reported hot band spectra of 8 different vibrational modes of HCO^+ . Works focused on the higher energy isomer, HOC^+ , are much more rare. The first rotational spectrum³ has only been followed by the infrared detection of the ν_1 band of HOC^+ ,²⁰ the hot band transition ν_1 in $\nu_2 = 1$,²¹ and another hot band study starting in the ν_2 state by Amano and Maeda²². Both HCO^+ and HOC^+ were subject to numerous theoretical spectroscopic studies^{6,7,23–27} with an emphasis on the prediction of the spectral properties of the lowest vibrational bands. While the calculated vibrational band origins are consistent across the studies, at least for the low lying states, the predicted lifetimes of the ν_1 state of HCO^+ differ by up to an order of magnitude.

The abundance of HOC^+ , i.e., the $[\text{HCO}^+]/[\text{HOC}^+]$ ra-

[a] Dr. Miguel Jiménez-Redondo, prof. Dr. Paola Caselli, Dr. Pavol Jusko*
Max Planck Institute for Extraterrestrial Physics, Gießenbachstraße 1, 85748 Garching, Germany
E-mail: pjusko@mpe.mpg.de

[b] Liliia Uvarova, Dr. Petr Dohnal, Miroslava Kassayová
Department of Surface and Plasma Science, Faculty of Mathematics and Physics, Charles University, V Holešovičkách 2, Prague 18000, Czech Republic

tion, has been observed in dense molecular clouds,²⁸ in diffuse clouds,²⁹ towards photodissociation regions (PDRs),^{30,31} and towards the Galactic Center.³² It has also been used as a diagnostic tool, e.g., starburst energy feedback seen through HCO⁺ and HOC⁺ emission in NGC 253.³³ Although the HCO⁺/HOC⁺ column density ratio has been found anywhere between 1000 and 9000 toward dark clouds, it has been observed to be significantly smaller (50-400) toward PDRs and diffuse clouds, suggesting an efficient HOC⁺ formation in these warmer environments.

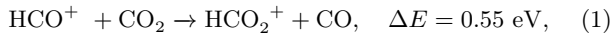
In this work, we present a study of the first overtone vibrational transition of the C–H and O–H stretching mode of HCO⁺ and HOC⁺. The measurements have been performed in a cryogenically cooled 22 pole ion trap using a laser induced reaction (LIR) action spectroscopy scheme. The setup allows us to determine the spectroscopic constants of the excited vibrational state for each ion as well as the corresponding radiative lifetimes and quenching rate coefficients with selected neutral partners.

Results and Discussion

Overtone Spectroscopy of HCO⁺/HOC⁺

The vibrational energy levels of both isomers are denoted by their vibrational quantum numbers, $\nu_1\nu_2\nu_3$, corresponding to the number of vibrational quanta in a given vibrational mode (following the notation by Neese *et al.*⁵). As we probe the C–H/O–H stretching mode only, we further abbreviate this notation such that $2\nu_1$ has the same meaning as 20^0_0 .

The laser induced reaction (LIR) technique³⁴ relies on the different reactivities of the upper and the lower state involved in the transition. The HCO⁺ spectra were measured by using the endothermic reaction with CO₂



and, similarly, using Ar for HOC⁺



where the endothermicities were calculated based on the proton affinities of the reactants taken from NIST.³⁵ These processes are best recognized by following the reaction paths in the energy level diagram Fig. 1. At room temperature and below, reactions (1) and (2) basically do not proceed due to the ions being almost exclusively in their ground vibrational state. The excitation of HCO⁺ or HOC⁺ to the $2\nu_1$ state and the “activation” of the reactions result then in an improved production of HCO₂⁺ or ArH⁺ ions, respectively.

Examples of obtained absorption lines are shown in Fig. 2. The measured overtone transitions from the ground vibrational state to $2\nu_1$ state for both HCO⁺ and HOC⁺ ions are summarized in Tab. 1. The upper and lower levels can be described by a Hamiltonian⁵

$$H = T_\nu + B_\nu(J+1) - D_\nu[J(J+1)]^2 + H_\nu[J(J+1)]^3, \quad (3)$$

where ν stands for the vibrational quantum numbers of a given level, T_ν is the vibrational term energy, J is the rotational quantum number, B_ν denotes the rotational constant, and D_ν and H_ν are the centrifugal distortion constants. The vibrational band origin for the $20^0_0 \leftarrow 00^0_0$ transition is $\omega_{2\nu_1} = T_{2\nu_1} - T_{0\nu_1}$.

The measured transition wavenumbers were fitted using Hamiltonian (3), where the spectroscopic constants for the lower state were fixed at values experimentally determined by Neese *et al.*⁵ for HCO⁺ and by Amano and Maeda²² for HOC⁺. The fitted spectroscopic constants are summarized in Tab. 2 and compared to the previous theoretical and experimental studies in Tab. 3. Note that two values, marked [N], acquired using cavity ring-down spectroscopy (CRDS), were excluded from the fit due to presence of other (unidentified) absorption features in immediate vicinity of the HCO⁺ transitions (see the dataset for more details).

The derived HCO⁺ spectroscopic constants are in a very good agreement with the hot band spectroscopy study by Neese *et al.*⁵ and also with recent quantum mechanical calculations.⁷ Although, in the HOC⁺ case, the older theoretical studies^{6,26,27} predicted the band origin $\omega_{2\nu_1}$ up to 30 cm⁻¹ away from the measured value, the newer spectroscopic constants estimated by Koput^{7,36} are in good agreement with the experiment (the predicted band origin $\omega_{2\nu_1}$ is within two $B_{2\nu_1}$ from the experimental one).

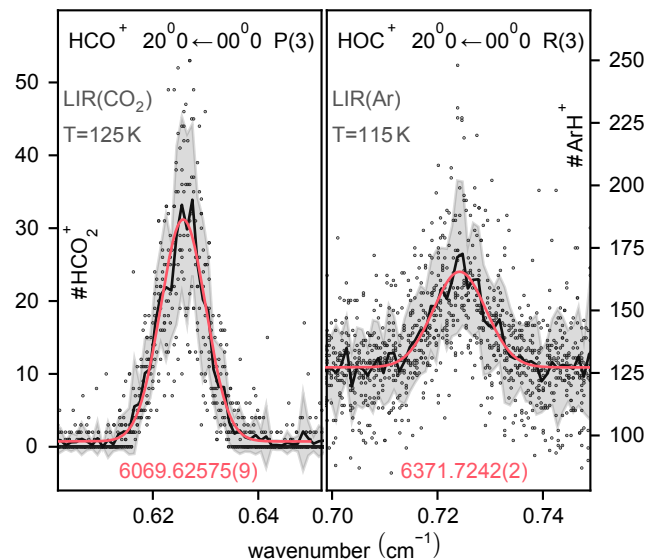


Figure 2. P(3) and R(3) lines of HCO⁺ and HOC⁺, respectively, measured by LIR technique in the 22 pole ion trap.

Radiative Lifetime of the $2\nu_1$ State

Measuring the overtone transitions while varying the number density of the LIR reactant allowed us to determine the radiative lifetime of the $2\nu_1$ state of HCO⁺ and HOC⁺. In the steady state, with low laser power, the number of HCO₂⁺ ions produced in the laser induced reaction (1) is proportional to the number of trapped HCO⁺ ions (predominantly in their ground vibrational state)

$$N_{\text{HCO}_2^+} = \frac{k_1[\text{CO}_2]r_1 N_{\text{HCO}^+}}{k_1[\text{CO}_2] + 1/\tau_{\text{rad}} + k_{\text{qM}}[M]} t, \quad (4)$$

where t is the irradiation time, r_1 corresponds to the rate of photon excitation to the $2\nu_1$ state, k_1 to the reaction rate coefficient of vibrationally excited HCO⁺ with CO₂, τ_{rad} is the time constant of the radiative deexcitation of the $2\nu_1$ state to lower lying vibrational levels, and k_{qM} is the collisional reaction rate coefficient for the quenching of the $2\nu_1$ state in collision with particle M . It is inherently assumed that k_1 is close to the Langevin collisional rate coefficient

Table 1. Measured transition wavenumbers for the $20^0_0 \leftarrow 00^0_0$ vibrational bands of HCO^+ and HOC^+ . Statistical error reported in parenthesis. The absolute accuracy of the wavemeter is better than 0.002 cm^{-1} .

HCO^+		HOC^+	
P(1)	6075.7093(1)	R(1)	6366.0286(5)
P(2)	6072.6892(1)	R(2)	6368.8965(5)
P(3)	6069.6258(1)	R(3)	6371.7242(2)
P(4)	6066.5171(1)	R(4)	6374.5134(3)
P(5) ^[c,N]	6063.3620(9)	R(8)	6385.2699(2)
P(6) ^[c,N]	6060.1689(2)	R(9)	6387.8592(2)
P(7) ^[c]	6056.9250(2)	R(10)	6390.4088(3)
P(8) ^[c]	6053.6385(3)	R(11)	6392.9174(3)

All frequencies in cm^{-1} . Fitted temperature (i. e. line width) varies between 130 – 210 K. [c] value obtained from the CRDS setup. [N] not included in the fit (see text).

Table 2. Spectroscopic constants, radiative lifetimes τ_{rad} , and quenching rate k_q for the 20^0_0 vibrational state of HCO^+ and HOC^+ ions derived in this work. The vibrational transition moment for the $20^0_0 \leftarrow 00^0_0$ transition and the reaction rate coefficients for the vibrational quenching of the 20^0_0 state in collision with different gases were determined only for HCO^+ ions. Statistical error is reported in parenthesis.

	HCO^+	HOC^+
$\omega_{2\nu_1}$	6078.68411(19)	6360.17630(26)
$B_{2\nu_1}$	1.465215(25)	1.472957(12)
$D_{2\nu_1}$	$3.56(44) \cdot 10^{-6}$	$4.03(11) \cdot 10^{-6}$
$H_{2\nu_1}$	–	$3.3(2.2) \cdot 10^{-10}$
$\langle 20^0_0 \mu 00^0_0 \rangle$	$0.0084(25)^{[a]}$	$\mu_{\text{HCO}^+} / 0.41(11)^{[b]}$
τ_{rad} (ms)	1.53(34)	1.22(34)
$k_{q\text{He}}^{[c]}$	5.6(1.0)	–
$k_{q\text{H}_2}^{[c]}$	580(110)	–
$k_{q\text{N}_2}^{[c]}$	640(40)	–

Spectroscopic constants in cm^{-1} . [a] lower estimate from the CRDS measurement in Debye. [b] derived from relative ion signal intensities in the 22 pole trap, see text, R_μ , Eq. (16). [c] in $10^{-12} \text{ cm}^3 \text{ s}^{-1}$.

and every collision of the $2\nu_1$ state of HCO^+ with CO_2 leads to HCO_2^+ , so the vibrational quenching induced by collisions with CO_2 can be neglected.

The radiative lifetime, τ_{rad} , is then obtained by fitting equation (4) to the dependence of the measured ratio of secondary (HCO_2^+ or ArH^+) to primary (HCO^+ or HOC^+) ions as a function of the number density of the probing gas (CO_2 or Ar) as shown in Fig. 3 for HCO^+ ions. The resulting radiative lifetime was $\tau_{\text{rad}} = 1.53 \pm 0.34 \text{ ms}$ for $\text{HCO}^+(2\nu_1)$ and $\tau_{\text{rad}} = 1.22 \pm 0.34 \text{ ms}$ for $\text{HOC}^+(2\nu_1)$ ions. The measurements were performed using the P(3) and R(3) lines for HCO^+ and HOC^+ , respectively, and the corresponding k_1 were calculated using polarisabilities from refs.^{37,38} Given that typical vibrational selection rules strongly favor transitions with vibrational quantum number changing by one, the measured radiative lifetimes probably

Table 3. Vibrational band origins and rotational constants of HCO^+ and HOC^+ obtained in previous theoretical and experimental studies.

$\omega_{2\nu_1}$	$B_{2\nu_1}$	Method/ Ref.
HCO^+		
6078.68411(19)	1.465215(25)	E [present]
6078.6839 ^[a]	1.4651993(13)	D ⁵
6079.8	1.46512	T ⁷
HOC^+		
6360.17630(26)	1.472957(12)	E [present]
6362.3	1.4736	T ³⁶
6391.5 ^[a]	1.4464 ^[a]	T ⁶
6377.9	1.4707 ^[a]	T ^{25,26}
6390.5		T ²⁷

Spectroscopic constants in units of cm^{-1} . Method: T – theory, E – experiment, D – derived from experimental data (fundamental + hot-band spectra). [a] Values calculated from published spectroscopic constants.

pertain to the transition $20^0_0 \rightarrow 10^0_0$ (note that the 10^0_0 level is endothermic in reaction with CO_2 (for HCO^+) as well as Ar (for HOC^+), i. e., it is not probed in the selected LIR schemes).

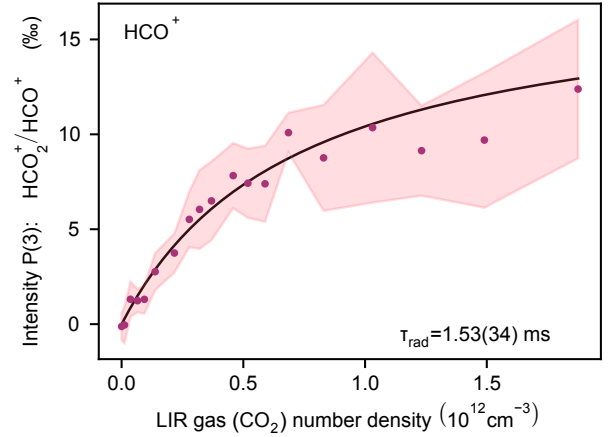


Figure 3. Determination of the τ_{rad} for HCO^+ from the increase of the LIR signal as a function of CO_2 number density in the trap using Eq. (4).

To our best knowledge, there are no experimental or theoretical data on the radiative lifetimes of the $2\nu_1$ states of either HCO^+ or HOC^+ . An approximate comparison with present data can be done applying the $1/\nu$ scaling law,¹⁶ i. e., that the lifetime of the $2\nu_1$ state should be about half of the $1\nu_1$ state. The predicted lifetimes for the $1\nu_1$ state of HCO^+ range from 0.4 ms²⁷ to 4.46 ms²³ with the majority of the studies closer to the upper value (e. g. 3.9 ms²⁴ or 3.7 ms⁶). Keim *et al.*¹⁵ in their DLASFIB (direct laser absorption in a fast ion beam) experiment¹⁵ measured an absolute vibrational band intensity that corresponds to a lifetime of $5.9 \pm 0.9 \text{ ms}$ for the $1\nu_1$ state of HCO^+ . Considering the aforementioned $1/\nu$ scaling law, the value of τ_{rad} for the $2\nu_1$ state of HCO^+ measured in the present experiment is thus within experimental error, comparable to that predicted for the $1\nu_1$ state by theoretical calculations,^{6,23,24} and lower than the value that could be extrapolated from

the experiment by Keim *et al.*¹⁵.

For HOC^+ ions, only theoretical data on vibrational lifetimes are available. Kraemer and Špirko²⁷ predicted the lifetime of the $1\nu_1$ state of HOC^+ to be 0.4 ms, very close to the value they calculated for the same transition in HCO^+ . Slightly higher values were reported by Rogers and Hillman²³ (0.6 ms), Botschwina²⁴ (0.7 ms) and Martin *et al.*⁶ (0.7 ms). These results are substantially lower than the value obtained in present experiment with the lifetime of the $2\nu_1$ state of HOC^+ re-scaled by the $1/\nu$ law. As this scaling law is valid for the harmonic approximation, it is difficult to distinguish whether the apparently longer than predicted radiative lifetime is due to anharmonic contributions to the wavefunctions or due to coupling to the other vibrational levels. Note that the scaling law is an approximation only, e.g., a deviation from the $1/\nu$ scaling by a factor of two was observed for the higher bending modes of DCO^+ in an ion storage ring study.³⁹

Collisional Quenching of $\text{HCO}^+(2\nu_1)$

In order to determine the rate coefficients for the quenching of the $2\nu_1$ vibrational state of HCO^+ in collisions with different species, the number density of the probing gas (CO_2) was kept constant and the number density of the collisional partner was varied over several orders of magnitude. The measured dependence of the ratio of secondary HCO_2^+ to primary HCO^+ ions as a function of the quenching partner number density at a temperature of 125 K is shown in Fig. 4. The quenching reaction rate coefficients k_{qM} for the particular species M were obtained by fitting the data in Fig. 4 using equation (4) where τ_{rad} was kept constant (at the value obtained in present study, 1.53 ± 0.34 ms). The resulting fitted reaction rates, summarized in Tab. 2, show that the quenching of the $2\nu_1$ vibrational state of HCO^+ by molecular gases H_2 , and N_2 , is two orders of magnitude more efficient than quenching by atomic He. It is important to note that the number density of the LIR reactant (CO_2) has to be chosen so that the LIR signal is high enough but at the same time not in saturation mode, i. e., somewhere in the first third of the curve shown in Fig. 3. In our quenching experiment, this value was ca. $3 \cdot 10^{11} \text{ cm}^{-3}$. The sensitivity to the changes of CO_2 number density (change by 20%) is shown on two different traces for He quenching. The method seems to be reliable, as implied by Eq. (4), as long as the CO_2 number density is not too large.

When the quenching partner is a molecule, its rovibrational structure makes vibrational energy transfer (V-V) possible,⁴⁰ in addition to vibration-to-translation (V-T). This V-V transfer is a resonant process, and HCO^+ possesses three normal modes with vibrational frequencies of $\nu_1 = 3089 \text{ cm}^{-1}$, $\nu_2 = 831 \text{ cm}^{-1}$, and $\nu_3 = 2183 \text{ cm}^{-1}$,⁷ thus, there are many possible vibrational states where HCO^+ can end up after a collision with a quenching gas (see Figure 1). Therefore, it can be expected that the measured quenching coefficients for collisions with molecular gases will have higher values than those that are typically obtained for vibrationally excited diatomic ions.^{40,41} In fact, the measured quenching coefficients $k_{q\text{H}_2} = 5.8 \pm 1.1 \cdot 10^{-10} \text{ cm}^3 \text{ s}^{-1}$ and $k_{q\text{N}_2} = 6.4 \pm 0.4 \cdot 10^{-10} \text{ cm}^3 \text{ s}^{-1}$ are close to the corresponding Langevin collisional rates of $1.5 \cdot 10^{-9} \text{ cm}^3 \text{ s}^{-1}$ and $8.2 \cdot 10^{-10} \text{ cm}^3 \text{ s}^{-1}$, respectively.

In an ion trap study by Schlemmer *et al.*⁴², the collisional quenching relaxation of antisymmetric C-H stretch mode ν_3

of C_2H_2^+ with H_2 has been estimated using a fit of a kinetic model to the number of reaction product as a function of H_2 number density as $1.3 \cdot 10^{-9} \text{ cm}^3 \text{ s}^{-1}$. Their approach could be described as more sophisticated in comparison with the one presented in this work, as the applied LIR scheme $\text{C}_2\text{H}_2^+(\nu_3=1) + \text{H}_2 \rightarrow \text{C}_2\text{H}_3^+ + \text{H}$ was not a simple proton transfer, i. e., the assumption of the Langevin behaviour did not hold and the reaction rate of the excited state had to be investigated concurrently. Their simulation also showed, that the quenching rate with H_2 was a “substantial fraction (0.81 – 0.87) of the Langevin rate”.

Atomic helium seems to be surprisingly efficient at quenching the $2\nu_1$ state of HCO^+ with $k_{q\text{He}} = 5.6 \pm 1.0 \cdot 10^{-12} \text{ cm}^3 \text{ s}^{-1}$. The weak helium-ion interaction potential often results in small ($< 10^{-15} \text{ cm}^3 \text{ s}^{-1}$ at 300 K) deexcitation rates as was observed, e.g., for N_2^+ and NO^+ .^{40,43} Even smaller reaction rate coefficients were predicted for low temperature collisional quenching of diatomic anions (CN^- , C_2^-) by helium.^{44,45} Wisthaler *et al.*⁴⁶ reported a rate coefficient of $1.3 \cdot 10^{-13} \text{ cm}^3 \text{ s}^{-1}$ for the quenching of vibrationally excited HCN^+ and DCN^+ ions in collision with helium at a collisional energy corresponding to a temperature of 1500 K, noting that the quenching reaction rate coefficient fell down below $10^{-14} \text{ cm}^3 \text{ s}^{-1}$ at lower energies.

The HCO^+ -He potential energy surface has a minimum of approximately 300 cm^{-1} below the dissociation limit.⁴⁷ For comparison, the N_2^+ -He system has minimum of only 140 cm^{-1} ⁴⁸ (with a corresponding vibrational quenching reaction rate coefficient of $1 \cdot 10^{-15} \text{ cm}^3 \text{ s}^{-1}$) and the O_2^+ -Ar system has a lowest dissociation energy of 765 cm^{-1} ⁴⁹ and the reported quenching coefficient for the $\nu = 1$ state of O_2^+ was $1 \cdot 10^{-12} \text{ cm}^3 \text{ s}^{-1}$.⁴¹ We note that it is very hard to predict the magnitude of the quenching coefficient based only on the interaction potentials and the polarisability of the neutral without a full quantum mechanical calculation.⁴⁵

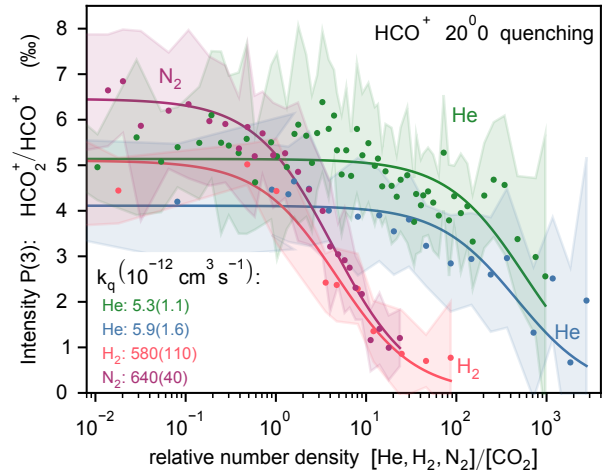


Figure 4. Determination of the quenching rate k_q for HCO^+ with He, H_2 , and N_2 from the decrease of the LIR signal as a function of the number density of the quenching partner in the trap using Eq. (4). The two different data sets for He, acquired with $> 20\%$ difference in the CO_2 LIR reactant number density, demonstrate the robustness of the technique.

Transition Dipole Moments for $20^0_0 \leftarrow 00^0_0$ Transition of HCO^+ and HOC^+

In order to estimate the value of the integrated molar infrared intensity of absorption γ for the $20^0_0 \leftarrow 00^0_0$ transition of HCO^+ in the Stationary Afterglow with Cavity Ring-Down Spectrometer (SA-CRDS) apparatus, we have followed the approach used for H_3^+ ions by Shapko *et al.*⁵⁰. Aided by a chemical kinetics model, the experimental conditions were set to maximize the amount of HCO^+ . The measured absorption signal can then be compared to the value of the electron number density determined at the same time in the afterglow by microwave diagnostics. Using the P(4), P(7) and P(8) transitions of HCO^+ , the obtained lower estimate for the molar infrared intensity of absorption was $\gamma = 18 \pm 5 \text{ cm}^2 \cdot \text{mol}^{-1}$, corresponding to a vibrational transition moment $\langle 20^0_0 | \mu | 00^0_0 \rangle = 0.0084 \pm 0.0025 \text{ D}$. This is lower than the value of $\gamma = 23.7 \text{ cm}^2 \cdot \text{mol}^{-1}$ predicted by Botschwina²⁴. The measurements were performed at temperatures of 80 K and 170 K and the H_2 and CO number densities were varied in the range of $5 \cdot 10^{13} - 5 \cdot 10^{15} \text{ cm}^{-3}$ with helium buffer gas pressure in the range of 500 to 1000 Pa. The stated error arises mainly from the estimated uncertainty of the electron number density determination.

Although it is inherently difficult to derive absolute intensities in an action spectroscopy experiment in an ion trap, relative evaluation is possible. We show how to correctly assess the relative intensities of two different species in a LIR action spectra in Eqs. (15–19). For high number densities of LIR probing gas and no quenching, equation (4) simplifies to

$$\begin{aligned} N_{\text{HCO}_2^+} / N_{\text{HCO}^+} &= \rho_1 = r_1 (\text{HCO}^+) t, & \text{for } \text{HCO}^+ \\ N_{\text{ArH}^+} / N_{\text{HOC}^+} &= \rho_2 = r_1 (\text{HOC}^+) t. & \text{for } \text{HOC}^+ \end{aligned} \quad (5)$$

The measured values were $\rho_1 = 0.0099 \pm 0.0013$ from the P(3) line of HCO^+ at 125 K, and $\rho_2 = 0.025 \pm 0.005$ from the R(3) line of HOC^+ at 115 K, at the same trapping time $t = 1.7 \text{ s}$. In the latter case, the chemical probing by $^{15}\text{N}_2$ has shown that only ca. 70 % of all ions with mass 29 m/z were HOC^+ , i. e., ρ_2 has to be increased accordingly. Assuming that Herman-Wallis factors are close to unity for both HCO^+ and HOC^+ , the resulting calculated ratios for the Einstein A coefficients (Eq. (16)) and vibrational transition moment squared (Eq. (19)) are $R_A = 0.48 \pm 0.10$ and $R_\mu = 0.41 \pm 0.11$. The stated uncertainty is only the statistical error. Systematic uncertainties arise mainly from the completely unknown overlap of the laser beam (different light sources/optics/path for both species) with the ion cloud in the trap. Even though $\text{HCO}^+/\text{HOC}^+$ have the same m/z , the distribution of the ions inside the trap will most probably differ, since neither effective potential V^* , nor the number of ions were the same, and on top, in case of HOC^+ , also the presence of the dominant lighter C^+ ion will play a significant role. Therefore, the results of this relative intensity determination technique are only illustrative, as we are unable to provide a reliable confidence interval.

Conclusions

We present the first spectra of the $2\nu_1$ overtone transition of HCO^+ and HOC^+ . The availability of this data and cheap

telecommunication laser diodes opens up the possibility of very cheap monitoring of these two isomers in any optically thin environment or in emission. Although the accuracy of the theoretical prediction of the HOC^+ band origin by Koput³⁶ is in the cm^{-1} range, we hope that the experimental spectroscopic constants will be helpful for further improvement of the *ab initio* theoretical models.

We explore the versatility of the cryogenic ion trapping technology and present a technique to improve the LIR action spectroscopy for very weak signals into a background free action spectroscopic method, by actively removing the background in the ion signal by selective m/z ejection from the trap. Furthermore, we extensively describe the method of determination of radiative lifetimes, τ_{rad} , and quenching reaction rates, k_q , and its caveats inside an ordinary 22 pole rf trap, easily applicable to a plethora of molecular ions.

Although similar experiments have been done in the past, e. g., τ_{rad} in an ICR,^{16,51} or measurements of quenching reaction rates for various, mainly diatomic, ions,^{41,43,45,52} this data exist only for a select few systems. Moreover, there are not many experiments focused on higher lying vibrational levels. The collisional quenching rates are needed for the treatment of the molecular emission lines in astronomy. We aspire to stimulate further study of τ_{rad} , and quenching rates for more ion molecular systems, as well as for the different transitions, e. g., different vibrational modes (bending, stretching, fundamentals, overtones etc.).

Last but not least, our quenching technique only shows the removal of the vibrational excitation in the molecular ion. We can not estimate what happened with the energy, whether it redistributed towards translational energy or into internal excitation of the quenching neutral molecule. These fundamental ion-molecule processes are not only of interest for astrophysics, but also closely related to action spectroscopy technology, i. e., LOS (leak-out spectroscopy) scheme,⁵³ where only the kinetic energy release is monitored in a quenching event. Consequently, a study of one system by both techniques could provide a full picture of energy distribution in the de-exciting collision.

Experimental Section

The measurements have been predominantly conducted in the CCIT 22 pole rf cryogenic trap setup,⁵⁴ with the exception of the P(5)–P(8) transitions of the HCO^+ ion acquired in the CRDS setup.⁵⁵ The experimental setups are extensively described in the references provided, we will only focus on particular improvements of the 22 pole trap setup needed for this experiment (the CRDS setup has been used without any modifications).

22 Pole Trap Setup

The 22 pole trap setup CCIT⁵⁴ consists of a storage ion source, quadrupole mass filter used to select the mass of the ion to be stored in the trap, the 22 pole trap mounted on variable temperature cryostat and a mass sensitive detection system. Each data point in the experiment, i. e., ion production, trapping, storage/ irradiation/ LIR reaction and detection, is acquired in a 3 s cycle time.

HCO^+ was produced directly from CO and H_2 precursor gases using electron bombardment in the storage ion source,⁵⁶ where the produced ions have many collisions with

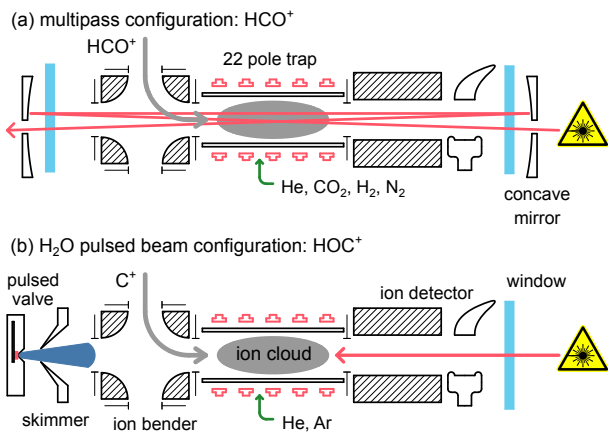
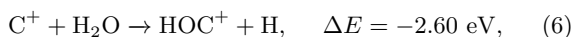


Figure 5. Experimental setup for a laser multi-pass configuration (HCO⁺ experiments – (a)), and an on axis molecular beam configuration (HOC⁺ experiments – (b)). Not to scale. For a detailed description of the experiment see ref. ⁵⁴

both CO and H₂, assuring dominant production of the lowest isomer. Subsequently, HCO⁺ was mass selected in a quadrupole filter and injected into the trap, where a short intense He pulse was used to trap it and provide collisional cooling into the ground state (see Fig. 5(a)).

In order to produce HOC⁺ in sufficient quantities, the following ion-molecule reaction⁵⁷ inside the trap was used



The C⁺ ion was produced in the ion source from CH₄ precursor gas using electron bombardment, mass selected and injected into the trap, where a short intense He pulse was used to trap and provide collisional cooling. Subsequently, an intense water pulse from the side of the trap (on the axis, ca. 200 ms long) was used to convert approx. 1/3 of the C⁺ ions into mass 29 m/z (HCO⁺ and HOC⁺) (see Fig. 5(b)). The on axis water beam had to be used to avoid the freezing of the water molecules at temperatures < 200 K. The ratio of the HOC⁺ to HCO⁺ ions was determined using proton transfer to ¹⁵N₂ as a chemical probing reaction. This reaction is exothermic for the HOC⁺ reactant only (see Fig. 1. Note that ¹⁴N₂H⁺ has the same mass as HOC⁺). This method of HOC⁺ production and isomer fraction determination has been recently described by Yang *et al.*⁵⁸. The gas pulses into the trap, as well as on the axis, are delivered using a custom built piezo element actuated valves, operated at the resonant frequency of a few kHz.

In both cases, following the ion preparation/ trapping, the ions are left stored in the trap for a predetermined time (1.75 s), during which the IR radiation can excite the ions in the ground state. The probing reactant gas (CO₂ in the case of HCO⁺ or Ar in the case of HOC⁺ spectroscopy) is flowing directly into the trap freely, maintaining a constant number density therein during the whole cycle time. Neither of the products of the LIR processes (1) and (2), HCO₂⁺ or ArH⁺, can undergo any significant further reaction inside the trap and thus accumulate until being detected at the end of the cycle. In the spectroscopy experiment, the wavelength of the laser radiation is scanned by a small step after every single data point taken and the spectrum as seen in Fig. 2 is acquired.

In case of the radiative lifetime experiment and quen-

ing experiment (Figs. 3, 4), the light wavelength is kept constant (on resonance), while the number density of the probing gases has to be varied using a variable leak valve. The pressure inside the vacuum vessel has been recorded using a Bayard-Alpert ion gauge (calibrated by an absolute pressure baratron gauge), the temperature transpiration effect was taken into account to accurately determine the number density in the trap (for details see ref. ⁵⁴).

We exclusively used continuous wave fiber pigtailed telecommunication grade distributed feedback (DFB) laser diodes FLPD-1647-07-DFB-BTF (HCO⁺ P(1)–P(4)), QDFBLD-1650-5 (HCO⁺ P(5)–P(6)), NX8570SD654Q-55 (HOC⁺ R(8)–R(11)), and QDFBLD-1570-20 (HOC⁺ R(1)–R(4)). A small part of the light has been split (fiber beam splitter, 1%) and fed into the WA-1650 (EXFO) wavemeter, with an absolute accuracy better than 0.3 ppm at 1500 nm. The majority of the light was guided into the trap using an adjustable focus collimator. Since the laser diode power for the HCO⁺ experiment was only ca. 7 mW, we decided to use a Pfund cell (two spherical mirrors $f = 750$ mm with a central $\phi 1.5$ mm hole) in a 3-pass configuration, effectively multiplying the power inside the trap by a factor of ≈ 2.5 (see Fig. 5(a)). The radiation power has been regularly monitored with a Ge photodiode.

Mass Selective Ejection – Zero Background Spectroscopy

The ions coming from the source can easily be mass selected to contain only the m/z ion of interest. The ion (HCO⁺) is consequently injected into the trap, where the stopping He pulse slows the ion down and removes its internal energy. However, if some other gas, e. g., probing gas (CO₂), is present in the trap, some of the incoming ions will collide with it prior to thermalisation (kinetic, internal degrees of freedom) and undergo a chemical reaction (product HCO₂⁺). As a consequence, it is impossible to fill the trap containing a probing gas and not produce any of the ions which are detected in the LIR scheme. This is usually of no concern for fundamental vibrational spectroscopy, where the absorption rates are usually two orders of magnitude stronger than for overtone vibrational transitions and the “injection” only creates a few percent of the total ions detected in the LIR scheme.

Fortunately, in this work, the products of the LIR reaction (HCO₂⁺: 45 m/z , ArH⁺: 41 m/z) are significantly heavier than the ions of interest 29 m/z . Therefore, we can vary the effective potential V^* in the trap, by lowering the driving amplitude V_0 for few hundred of ms, to achieve conditions where the higher mass ion is no longer efficiently trapped, effectively cleaning the trap from masses higher than a set threshold of ca. 40 m/z (see Gerlich⁵⁶ for details on trap technology). The effect of this technique can be best observed on the left panel of Fig. 2, where the off resonance background signal of HCO₂⁺ is essentially 0 (note that the value is not kept at 0 on purpose, since it is difficult to spot any instrument malfunction while scanning without having any signal at all).

The same technique is applied for the HOC⁺ spectroscopy, where the few hundred ms long ejection time additionally allows the excited HOC⁺/HCO⁺, produced in a strongly exothermic reaction (6), to radiatively decay to its vibrational ground state. Unfortunately, in this configuration, some of the water vapor and precursor ion C⁺ is always present, effectively creating excited products of the reac-

tion (6) all the time. These can further react with the probing neutral Ar, even off HOC^+ resonance, and contaminate the trap with ArH^+ during the 1.75 s irradiation time. To provide some quantitative values, in case of HOC^+ experiment, the trap is operated at $f_0 = 19.5$ MHz and V_0 from 41 V (everything trapped) to 26 V (ejection of masses $> 40 m/z$). The change in effective potential $V^*(0.8 r_0)$ for mass 29 m/z is then $5.2 \rightarrow 2.1$ meV and respectively for mass 41 m/z it is $3.7 \rightarrow 1.5$ meV.

CRDS Setup

The SA-CRDS apparatus (Stationary Afterglow with Cavity Ring-Down Spectrometer) was utilized for the measurement of 4 line positions in this study. Originally developed for the determination of recombination rate coefficients for collisions of electrons with molecular ions,^{59,60} it was also used for measurements of the line positions of overtone transitions for several polyatomic ions.^{55,61}

The main diagnostic technique is a continuous wave modification of cavity ring-down spectroscopy based on a design by Romanini *et al.*⁶². The HCO^+ ions were produced in a pulsed microwave discharge (discharge power of ≈ 17 W, period of 4.9 ms, 40% duty cycle) ignited in a He/Ar/H₂/CO mixture with reactant number densities of $8 \cdot 10^{17}/2 \cdot 10^{14}/4 \cdot 10^{14}/4 \cdot 10^{14} \text{ cm}^{-3}$. The discharge tube made of fused silica was immersed in liquid nitrogen.

We employed a model of chemical kinetics and varied the reactant number densities by almost an order of magnitude to maximize the number of HCO^+ ions in the discharge and afterglow plasma.

Radiative Deexcitation/ Collisional Quenching Derivation

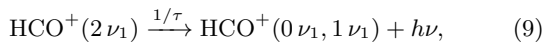
In the following, we derive Eq. (4), used for the determination of τ_{rad} and k_q , for the $\text{HOC}^+(2\nu_1)$ case. The technique can be applied on any analogous LIR system and transition (fundamental, overtone etc.), e. g., for HOC^+ ions with Ar probing gas, etc. For simplicity, let's consider only the most important processes involving HCO^+ ions in the 22 pole rf trap:

1. Overtone excitation



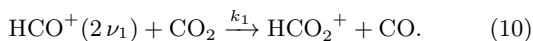
where r_1 is the rate for excitation from the vibrational ground state by two vibrational quanta in the stretching mode ν_1 . It depends on the corresponding transition line strength, the intensity of the laser and on the overlap between the ion cloud in the trap and the laser beam.

2. Deexcitation of the vibrationally excited HCO^+ ions to lower states



here $1/\tau = 1/\tau_{\text{rad}} + 1/\tau_q$, with τ_{rad} representing spontaneous emission, and τ_q deexcitation due to collisions with another particle. In our particular case, it can be safely assumed that τ_{rad} is mainly given by the transition to the $1\nu_1$ state.

3. Proton transfer in reaction with the probing gas



The corresponding rate equations for $\text{HCO}^+(2\nu_1)$ and HCO_2^+ can then be written as

$$\frac{dN_{\text{HCO}^+(2\nu_1)}}{dt} = -k_1 N_{\text{HCO}^+(2\nu_1)} [\text{CO}_2] - \frac{1}{\tau} N_{\text{HCO}^+(2\nu_1)} + r_1 N_{\text{HCO}^+(0\nu_1)}, \quad (11)$$

$$\frac{dN_{\text{HCO}_2^+}}{dt} = k_1 N_{\text{HCO}^+(2\nu_1)} [\text{CO}_2], \quad (12)$$

where N_i denotes number of ions of species i in the trap.

By utilising the steady-state approximation, we can express $N_{\text{HCO}^+(2\nu_1)}$ from equation (11) and insert it into equation (12). After simple integration we obtain

$$N_{\text{HCO}_2^+} = \frac{k_1 [\text{CO}_2] r_1 N_{\text{HCO}^+(0\nu_1)} t}{k_1 [\text{CO}_2] + 1/\tau} \quad (13)$$

for the number of detected HCO_2^+ ions, where t is trapping time. Noting that $1/\tau = 1/\tau_{\text{rad}} + 1/\tau_q$ and that $1/\tau_q = k_{qM}[\text{M}]$, equation (13) can be rewritten as

$$N_{\text{HCO}_2^+} = \frac{k_1 [\text{CO}_2] r_1 N_{\text{HCO}^+(2\nu_1)} t}{k_1 [\text{CO}_2] + 1/\tau_{\text{rad}} + k_{qM}[\text{M}]}, \quad (14)$$

where k_{qM} is the reaction rate coefficient for the quenching of the $2\nu_1$ state of HCO^+ in collisions with particles M. This relation can be used to determine the lifetime of spontaneous emission by varying the LIR reactant number density, as well as to evaluate the quenching rate by varying the number density of the quenching particles [M] (provided τ_{rad} is known), from the measured LIR signal, $N_{\text{HCO}_2^+}/N_{\text{HCO}^+(0\nu_1)}$, as a function of the respective number density.

Relative Transition Intensities in Action Spectroscopy

In saturation conditions, i. e., conditions with high LIR reactant gas number density such that neither τ_{rad} nor quenching play a role, the intensity of the LIR signal, defined by Eq. (14), reduces to Eq. (5), i. e., $\rho = r_1 t$. The rate of excitation to the $2\nu_1$ vibrational state is proportional to the laser power and to the Einstein coefficient for given transition. Following the derivation in refs.^{50,63} and assuming a thermal population of states, the Einstein coefficient $A_{J\nu J'\nu'}$ for spontaneous emission between two rovibrational states of HCO^+ is proportional to the measured ratio ρ of the numbers of secondary (HCO_2^+ or ArH^+) and primary (HCO^+ or HOC^+) ions obtained at high probing gas number densities

$$A_{J\nu J'\nu'} \sim \rho \frac{8\pi\nu^2 c Q(T)}{g_u} \exp \frac{E}{k_B T} \sqrt{\frac{\pi}{4 \ln 2}} w/I, \quad (15)$$

where ν is the transition wavenumber, c is speed of light, k_B is the Boltzmann constant, $Q(T)$ is the partition function at temperature T , g_u denotes the statistical weight of the upper state, E is the energy of the lower state of the transition, w is the full width at half maximum (FWHM) of the Doppler broadened line, and I is the number of photons passing through the trap per second. The ratio between the Einstein coefficients of two rovibrational transitions is then

$$R_A = \frac{A_1}{A_2} = \frac{\rho_1 \nu_1^2 w_1 g_{11} g_{u2} P_2 I_2}{\rho_2 \nu_2^2 w_2 g_{12} g_{u1} P_1 I_1}, \quad (16)$$

where the subscripts 1 and 2 distinguish between the transitions and P is the thermal population of the lower state with

statistical weight g_l . The state to state transition dipole moment squared $\langle Jv|\mu|J'v'\rangle^2$ is connected to the corresponding vibrational transition moment $\langle v|\mu|v'\rangle$ through the relation⁶⁴

$$\langle Jv|\mu|J'v'\rangle^2 = \langle v|\mu|v'\rangle^2 S_J^{\Delta J} F(m), \quad (17)$$

where $S_J^{\Delta J}$ and $F(m)$ are Hönl-London and Herman-Wallis factor, respectively. Given that⁶³

$$A_{JvJ'v'} = \frac{64\pi^4}{3h} \nu^3 \frac{g_l}{g_u} \langle Jv|\mu|J'v'\rangle^2 \times 10^{-36} \text{ s}^{-1}, \quad (18)$$

with h in cm^2gs , ν in cm^{-1} and $\langle Jv|\mu|J'v'\rangle$ in Debye, it follows that

$$R_\mu = \frac{\langle v|\mu|v'\rangle_{\text{HCO}^+}^2}{\langle v|\mu|v'\rangle_{\text{HOC}^+}^2} = \frac{\rho_1 w_1 \nu_2 P_2 I_2 S_{J_2}^{\Delta J} F_2(m)}{\rho_2 w_2 \nu_1 P_1 I_1 S_{J_1}^{\Delta J} F_1(m)}. \quad (19)$$

Acknowledgements

This work was supported by the Max Planck Society, the Czech Science Foundation (Grant Nos. GACR 23-05439S and GACR 22-05935S), and the Charles University (Grant Nos. GAUK 337821 and GAUK 332422). L.U. acknowledges support by the COST Action CA21101. The authors gratefully acknowledge the work of the electrical and mechanical workshops and engineering departments of the Max Planck Institute for Extraterrestrial Physics.

Conflict of Interest

The authors report there are no competing interests to declare.

Additional Information

The data that support the findings of this study are openly available in Zenodo at <https://doi.org/10.5281/zenodo.10473481>, reference number 10473481.

Keywords: astrophysics • cryogenic ion trap • ion-molecule interactions • isomers • vibrational spectroscopy

References

- [1] D. Buhl and L. E. Snyder, *Nature*, 1970, **228**, 267–269, DOI: [10.1038/228267a0](https://doi.org/10.1038/228267a0).
- [2] R. C. Woods, T. A. Dixon, R. J. Saykally and P. G. Szanto, *Phys. Rev. Lett.*, 1975, **35**, 1269–1272, DOI: [10.1103/PhysRevLett.35.1269](https://doi.org/10.1103/PhysRevLett.35.1269).
- [3] C. S. Gudeman and R. C. Woods, *Phys. Rev. Lett.*, 1982, **48**, 1344–1348, DOI: [10.1103/PhysRevLett.48.1344](https://doi.org/10.1103/PhysRevLett.48.1344).
- [4] R. C. Woods, C. S. Gudeman, R. L. Dickman, P. F. Goldsmith, G. R. Huguenin, W. M. Irvine, A. Hjalmarson, L. A. Nyman and H. Olofsson, *ApJ*, 1983, **270**, 583–588, DOI: [10.1086/161150](https://doi.org/10.1086/161150).
- [5] C. F. Neese, P. S. Kreynin and T. Oka, *The Journal of Physical Chemistry A*, 2013, **117**, 9899–9907, DOI: [10.1021/jp312879f](https://doi.org/10.1021/jp312879f).
- [6] J. M. L. Martin, P. R. Taylor and T. J. Lee, *The Journal of Chemical Physics*, 1993, **99**, 286–292, DOI: [10.1063/1.465806](https://doi.org/10.1063/1.465806).
- [7] J. Koput, *The Journal of Chemical Physics*, 2019, **150**, 154307, DOI: [10.1063/1.5089718](https://doi.org/10.1063/1.5089718).
- [8] C. G. Freeman, J. S. Knight, J. G. Love and M. J. McEwan, *International Journal of Mass Spectrometry and Ion Processes*, 1987, **80**, 255–271, DOI: [10.1016/0168-1176\(87\)87034-9](https://doi.org/10.1016/0168-1176(87)87034-9).
- [9] A. J. Chalk and L. Radom, *Journal of the American Chemical Society*, 1997, **119**, 7573–7578, DOI: [10.1021/ja971055c](https://doi.org/10.1021/ja971055c).
- [10] C. S. Gudeman, M. H. Begemann, J. Pfaff and R. J. Saykally, *Phys. Rev. Lett.*, 1983, **50**, 727–731, DOI: [10.1103/PhysRevLett.50.727](https://doi.org/10.1103/PhysRevLett.50.727).
- [11] T. Amano, *The Journal of Chemical Physics*, 1983, **79**, 3595–3595, DOI: [10.1063/1.446216](https://doi.org/10.1063/1.446216).
- [12] P. Davies and W. Rothwell, *The Journal of Chemical Physics*, 1984, **81**, 5239–5240, DOI: [10.1063/1.447688](https://doi.org/10.1063/1.447688).
- [13] K. Kawaguchi, C. Yamada, S. Saito and E. Hirota, *The Journal of Chemical Physics*, 1984, **82**, 1750–1755, DOI: [10.1063/1.448407](https://doi.org/10.1063/1.448407).
- [14] P. Davies, P. Hamilton and W. Rothwell, *The Journal of Chemical Physics*, 1984, **81**, 1598–1599, DOI: [10.1063/1.447889](https://doi.org/10.1063/1.447889).
- [15] E. R. Keim, M. L. Polak, J. C. Owrutsky, J. V. Coe and R. J. Saykally, *The Journal of Chemical Physics*, 1990, **93**, 3111–3119, DOI: [10.1063/1.458845](https://doi.org/10.1063/1.458845).
- [16] G. Mauclaire, J. Lemaire, M. Heninger, S. Fenistein, D. Parent and R. Marx, *International Journal of Mass Spectrometry and Ion Processes*, 1995, **149-150**, 487–497, DOI: [10.1016/0168-1176\(95\)04282-P](https://doi.org/10.1016/0168-1176(95)04282-P).
- [17] R. J. Foltynowicz, J. D. Robinson, E. J. Zückerman, H. G. Hedderich and E. R. Grant, *Journal of Molecular Spectroscopy*, 2000, **199**, 147–157, DOI: [10.1006/jmsp.1999.8014](https://doi.org/10.1006/jmsp.1999.8014).
- [18] V. Lattanzi, A. Walters, B. J. Drouin and J. C. Pearson, *The Astrophysical Journal*, 2007, **662**, 771, DOI: [10.1086/517602](https://doi.org/10.1086/517602).
- [19] B. M. Siller, J. N. Hodges, A. J. Perry and B. J. McCall, *The Journal of Physical Chemistry A*, 2013, **117**, 10034–10040, DOI: [10.1021/jp400570m](https://doi.org/10.1021/jp400570m).
- [20] T. Nakanaga and T. Amano, *Journal of Molecular Spectroscopy*, 1987, **121**, 502–504, DOI: [10.1016/0022-2852\(87\)90065-8](https://doi.org/10.1016/0022-2852(87)90065-8).
- [21] T. Amano, *Journal of Molecular Spectroscopy*, 1990, **139**, 457–460, DOI: [10.1016/0022-2852\(90\)90083-3](https://doi.org/10.1016/0022-2852(90)90083-3).
- [22] T. Amano and A. Maeda, *Journal of Molecular Spectroscopy*, 2000, **203**, 140–144, DOI: [10.1006/jmsp.2000.8158](https://doi.org/10.1006/jmsp.2000.8158).

- [23] J. D. Rogers and J. J. Hillman, *The Journal of Chemical Physics*, 1982, **77**, 3615–3626, DOI: [10.1063/1.444264](https://doi.org/10.1063/1.444264).
- [24] P. Botschwina, in *Ion and Cluster Ion Spectroscopy and Structure*, ed. J. P. Maier, Elsevier, Amsterdam, 1989, pp. 59–108.
- [25] M. Mladenovic and S. Schmatz, *The Journal of Chemical Physics*, 1998, **109**, 4456–4470, DOI: [10.1063/1.477049](https://doi.org/10.1063/1.477049).
- [26] M. Mladenović, *The Journal of Chemical Physics*, 2017, **147**, 114111, DOI: [10.1063/1.4998467](https://doi.org/10.1063/1.4998467).
- [27] W. P. Kraemer and V. Špirko, *Chemical Physics*, 2010, **373**, 170–180, DOI: [10.1016/j.chemphys.2010.04.018](https://doi.org/10.1016/j.chemphys.2010.04.018).
- [28] A. J. Apponi and L. M. Ziurys, *The Astrophysical Journal*, 1997, **481**, 800, DOI: [10.1086/304080](https://doi.org/10.1086/304080).
- [29] Liszt, H., Lucas, R. and Black, J. H., *A&A*, 2004, **428**, 117–120, DOI: [10.1051/0004-6361:20041649](https://doi.org/10.1051/0004-6361:20041649).
- [30] A. J. Apponi, T. C. Pesch and L. M. Ziurys, *The Astrophysical Journal*, 1999, **519**, L89, DOI: [10.1086/312096](https://doi.org/10.1086/312096).
- [31] Fuente, A., Rodriguez-Franco, A., Garcia-Burillo, S., Martin-Pintado, J. and Black, J. H., *A&A*, 2003, **406**, 899–913, DOI: [10.1051/0004-6361:20030712](https://doi.org/10.1051/0004-6361:20030712).
- [32] J. Armijos-Abendaño, J. Martín-Pintado, M. A. Requena-Torres, S. Martín and A. Rodríguez-Franco, *Monthly Notices of the Royal Astronomical Society*, 2014, **446**, 3842–3862, DOI: [10.1093/mnras/stu2271](https://doi.org/10.1093/mnras/stu2271).
- [33] N. Harada, S. Martín, J. G. Mangum, K. Sakamoto, S. Muller, K. Tanaka, K. Nakanishi, R. Herrero-Illana, Y. Yoshimura, S. Mühle, R. Aladro, L. Colzi, V. M. Rivilla, S. Aalto, E. Behrens, C. Henkel, J. Holdship, P. K. Humire, D. S. Meier, Y. Nishimura, P. P. van der Werf and S. Viti, *The Astrophysical Journal*, 2021, **923**, 24, DOI: [10.3847/1538-4357/ac26b8](https://doi.org/10.3847/1538-4357/ac26b8).
- [34] S. Schlemmer, T. Kuhn, E. Lescop and D. Gerlich, *International Journal of Mass Spectrometry*, 1999, **185–187**, 589–602, DOI: [10.1016/S1387-3806\(98\)14141-6](https://doi.org/10.1016/S1387-3806(98)14141-6).
- [35] P. J. Lindstrom and W. G. Mallard, *NIST Chemistry WebBook, NIST Standard Reference Database Number 69*, National Institute of Standards and Technology, Gaithersburg MD, 20899, 2023, DOI: [10.18434/T4D303](https://doi.org/10.18434/T4D303).
- [36] J. Koput, Private Communication, 2021.
- [37] R. Asher, D. Bellert, T. Buthelezi, V. Lewis and P. Brucati, *Chemical Physics Letters*, 1995, **234**, 113–118, DOI: [10.1016/0009-2614\(95\)00005-O](https://doi.org/10.1016/0009-2614(95)00005-O).
- [38] G. R. Alms, A. Burnham and W. H. Flygare, *The Journal of Chemical Physics*, 2008, **63**, 3321–3326, DOI: [10.1063/1.431821](https://doi.org/10.1063/1.431821).
- [39] R. Wester, U. Hechtfisher, L. Knoll, M. Lange, J. Levin, M. Scheffel, D. Schwalm, A. Wolf, A. Baer, Z. Vager, D. Zajfman, M. Mladenović and S. Schmatz, *The Journal of Chemical Physics*, 2002, **116**, 7000–7011, DOI: [10.1063/1.1461812](https://doi.org/10.1063/1.1461812).
- [40] E. E. Ferguson, *The Journal of Physical Chemistry*, 1986, **90**, 731–738, DOI: [10.1021/j100277a008](https://doi.org/10.1021/j100277a008).
- [41] H. Böhringer, M. Durup-Ferguson, E. Ferguson and D. Fahey, *Planetary and Space Science*, 1983, **31**, 483–487, DOI: [10.1016/0032-0633\(83\)90160-5](https://doi.org/10.1016/0032-0633(83)90160-5).
- [42] S. Schlemmer, E. Lescop, J. von Richthofen, D. Gerlich and M. A. Smith, *The Journal of Chemical Physics*, 2002, **117**, 2068–2075, DOI: [10.1063/1.1487373](https://doi.org/10.1063/1.1487373).
- [43] S. Kato, V. M. Bierbaum and S. R. Leone, *International Journal of Mass Spectrometry and Ion Processes*, 1995, **149–150**, 469–486, DOI: [10.1016/0168-1176\(95\)04283-Q](https://doi.org/10.1016/0168-1176(95)04283-Q).
- [44] B. P. Mant, F. A. Gianturco, R. Wester, E. Yurtsever and L. González-Sánchez, *Phys. Rev. A*, 2020, **102**, 062810, DOI: [10.1103/PhysRevA.102.062810](https://doi.org/10.1103/PhysRevA.102.062810).
- [45] B. Mant, E. Yurtsever, L. González-Sánchez, R. Wester and F. A. Gianturco, *The Journal of Chemical Physics*, 2021, **154**, 084305, DOI: [10.1063/5.0039854](https://doi.org/10.1063/5.0039854).
- [46] A. Wisthaler, A. Hansel, M. Schwarzmann, C. Scheiring, W. Lindinger and E. E. Ferguson, *The Journal of Chemical Physics*, 2000, **112**, 731–735, DOI: [10.1063/1.480644](https://doi.org/10.1063/1.480644).
- [47] F. Tonolo, L. Bizzocchi, M. Melosso, F. Lique, L. Dore, V. Barone and C. Puzzarini, *The Journal of Chemical Physics*, 2021, **155**, 234306, DOI: [10.1063/5.0075929](https://doi.org/10.1063/5.0075929).
- [48] S. Miller, J. Tennyson, B. Follmeg, P. Rosmus and H. Werner, *The Journal of Chemical Physics*, 1988, **89**, 2178–2184, DOI: [10.1063/1.455062](https://doi.org/10.1063/1.455062).
- [49] K. J. Catani, N. I. Bartlett, M. S. Scholz, G. Muller, P. R. Taylor and E. J. Bieske, *The Journal of Chemical Physics*, 2023, **159**, 024308, DOI: [10.1063/5.0152570](https://doi.org/10.1063/5.0152570).
- [50] D. Shapko, P. Dohnal, Štěpán Roučka, L. Uvarova, M. Kassayová, R. Plašil and J. Glosík, *Journal of Molecular Spectroscopy*, 2021, **378**, 111450, DOI: [10.1016/j.jms.2021.111450](https://doi.org/10.1016/j.jms.2021.111450).
- [51] M. Heninger, D. Lauvergnat, J. Lemaire, P. Boissel, G. Mauclaire and R. Marx, *International Journal of Mass Spectrometry*, 2003, **223–224**, 669–678, DOI: [10.1016/S1387-3806\(02\)00938-7](https://doi.org/10.1016/S1387-3806(02)00938-7).
- [52] S. Kato, V. M. Bierbaum and S. R. Leone, *The Journal of Physical Chemistry A*, 1998, **102**, 6659–6667, DOI: [10.1021/jp981679k](https://doi.org/10.1021/jp981679k).
- [53] P. C. Schmid, O. Asvany, T. Salomon, S. Thorwirth and S. Schlemmer, *The Journal of Physical Chemistry A*, 2022, **126**, 8111–8117, DOI: [10.1021/acs.jpca.2c05767](https://doi.org/10.1021/acs.jpca.2c05767).
- [54] P. Jusko, M. Jiménez-Redondo and P. Caselli, *Mol. Phys.*, 2024, **122**, e2217744, DOI: [10.1080/00268976.2023.2217744](https://doi.org/10.1080/00268976.2023.2217744).
- [55] P. Hlavenka, R. Plašil, G. Bánó, I. Korolov, D. Gerlich, J. Ramanlal, J. Tennyson and J. Glosík, *International Journal of Mass Spectrometry*, 2006, **255–256**, 170–176, DOI: [10.1016/j.ijms.2006.02.002](https://doi.org/10.1016/j.ijms.2006.02.002).

- [56] D. Gerlich, in *Adv. Chem. Phys.: State-Selected and State-to-State Ion-Molecule Reaction Dynamics*, ed. C.-Y. Ng and M. Baer, Wiley, New York, 1992, vol. LXXXII, pp. 1–176, DOI: [10.1002/9780470141397.ch1](https://doi.org/10.1002/9780470141397.ch1).
- [57] D. M. Sonnenfroh, R. A. Curtis and J. M. Farrar, *The Journal of Chemical Physics*, 1985, **83**, 3958–3964, DOI: [10.1063/1.449108](https://doi.org/10.1063/1.449108).
- [58] T. Yang, A. Li, G. K. Chen, Q. Yao, A. G. Suits, H. Guo, E. R. Hudson and W. C. Campbell, *Science Advances*, 2021, **7**, eabe4080, DOI: [10.1126/sciadv.abe4080](https://doi.org/10.1126/sciadv.abe4080).
- [59] P. Macko, G. Bánó, P. Hlavenka, R. Plašil, V. Poterya, A. Pysanenko, O. Votava, R. Johnsen and J. Glosík, *International Journal of Mass Spectrometry*, 2004, **233**, 299–304, DOI: [10.1016/j.ijms.2003.12.035](https://doi.org/10.1016/j.ijms.2003.12.035).
- [60] D. Shapko, P. Dohnal, M. Kassayová, v. Kálosi, S. Rednyk, v. Roučka, R. Plašil, L. D. Augustovičová, R. Johnsen, V. Špirko and J. Glosík, *The Journal of Chemical Physics*, 2020, **152**, 024301, DOI: [10.1063/1.5128330](https://doi.org/10.1063/1.5128330).
- [61] A. Kálosi, P. Dohnal, D. Shapko, Š. Roučka, R. Plašil, R. Johnsen and J. Glosík, *Journal of Instrumentation*, 2017, **12**, C10010, DOI: [10.1088/1748-0221/12/10/C10010](https://doi.org/10.1088/1748-0221/12/10/C10010).
- [62] D. Romanini, A. Kachanov, N. Sadeghi and F. Stoeckel, *Chemical Physics Letters*, 1997, **264**, 316–322, DOI: [10.1016/S0009-2614\(96\)01351-6](https://doi.org/10.1016/S0009-2614(96)01351-6).
- [63] L. Rothman, C. Rinsland, A. Goldman, S. Massie, D. Edwards, J.-M. Flaud, A. Perrin, C. Camy-Peyret, V. Dana, J.-Y. Mandin, J. Schroeder, A. McCann, R. Gamache, R. Wattson, K. Yoshino, K. Chance, K. Jucks, L. Brown, V. Nemtchinov and P. Varanasi, *Journal of Quantitative Spectroscopy and Radiative Transfer*, 1998, **60**, 665–710, DOI: [10.1016/S0022-4073\(98\)00078-8](https://doi.org/10.1016/S0022-4073(98)00078-8).
- [64] P. F. Bernath, *Spectra of Atoms and Molecules*, Oxford University Press, New York, 2005.